

Origins of

This content has been downloaded from IOPscience. Please scroll down to see the full text.

Download details:

IP Address: 128.138.41.170

This content was downloaded on 14/07/2015 at 11:17

Please note that terms and conditions apply.

## Origins of $k\phi$ errors for [001] GaAs/AlAs heterostructures

D. M. Wood<sup>1</sup>( $\sphericalangle$ ), A. Zunger<sup>1</sup>( $\sphericalangle$ ) and D. Gershoni<sup>2</sup>

<sup>1</sup> National Renewable Energy Laboratory - Golden, CO 80401, USA

<sup>2</sup> Department of Physics, Technion-Israel Institute of Technology - Haifa, 32000, Israel

(received 5 September 1995; accepted in final form 3 January 1996)

PACS. 73.20Dx { Electron states in low-dimensional structures (including quantum wells, superlattices, layer structures, and intercalation compounds).

PACS. 71.10+x { General theories and computational techniques (including many-body perturbation theory, density-functional theory, atomic sphere approximation methods, Fourier decomposition methods, etc.).

**Abstract.** { The  $k\phi$  method + envelope function combination used for semiconductor heterostructures is based on approximations dubious under some conditions. We directly compare 8-band  $k\phi$  with pseudopotential results for [001] GaAs/AlAs superlattices and quantum wells with all  $k\phi$  input parameters directly computed from bulk GaAs and AlAs pseudopotential bands. We find generally very good agreement for zone-center hole states within  $\gg 200$  meV of the GaAs valence band maximum, but i) systematic errors deeper in the valence band and ii) qualitative errors for even the lowest conduction bands with appreciable contributions from off- $j$  zinc-blende states. We trace these errors to inadequate  $k\phi$  description of *bulk* GaAs and AlAs band dispersion away from the zone center.

Nanostructures  $\gtrsim 100\text{\AA}$  in size were until recently [1] beyond reach of the atomistic electronic structure methods used for bulk crystals, *i.e.* *direct* solution of the Schrödinger equation

$$\left[ -\frac{\hbar^2}{2m} \nabla^2 + \sum_{i;\mathbf{R}_i} v_i(\mathbf{r} - \mathbf{R}_i) \right] \psi(\mathbf{r}) = E \psi(\mathbf{r}); \quad (1)$$

with the crystal potential  $V(\mathbf{r})$  here written as a superposition of screened atomic pseudopotentials  $v_i$  for atom species  $i$ . The spectroscopy of A/B heterostructures was instead interpreted [2] using an approach so common we term it the 'standard model' (SM): the  $k\phi$  method combined with the envelope function approximation (EFA). Although the SM has been eminently successful [3], even for ultrathin systems [4], approximations on which it is based compromise its description of heterostructures. Their impact has been partially masked by fitting of its parameters to experimental data, as described below. On general grounds one expects the SM to fail for short-period superlattices but would like to know *when* (for what thicknesses) and *how* (for which states) it fails. While detailed analyses of potential

(\*) Permanent address: Department of Physics, Colorado School of Mines, Golden, CO 80401 USA; e-mail: dmwood@physics.mines.edu

(\*\*) E-mail: alex.zunger@nrel.gov

pitfalls of the SM have appeared [5], the SM cannot assess its own validity. Evaluations of actual SM errors via non-SM methods, *e.g.* tight-binding [6], generally used input data (*e.g.* effective masses) from different sources and did not necessarily reflect SM deficiencies. Only by comparing direct solutions of the fully atomistic Schrödinger equation as in eq. (1) can such errors be systematically assessed. This approach is free of approximations made in the standard model, includes full-zone dispersion of all bands, and can predict complete Bloch wave functions. We use [001] (AlAs)<sub>n</sub>(GaAs)<sub>n</sub> superlattices for  $n \cdot 20$  and (GaAs)<sub>n</sub>/AlAs quantum wells to test the standard model against a direct pseudopotential approach (eq. (1)), with the former's input parameters computed from the latter to guarantee meaningful comparison. We trace systematic errors in the SM for *heterostructures* to inadequate description of dispersion of *bulk* bands in the Brillouin zone region where coupling to off- $j$  states is important.

For periodic systems the cell-periodic part  $u$  of the Bloch function  $\psi_{n\mathbf{k}} = \exp[i\mathbf{k} \cdot \mathbf{r}]u_{n\mathbf{k}}(\mathbf{r})$  may be expanded [7] about a reference point  $\mathbf{k}_0$ :

$$u_{n\mathbf{k}}(\mathbf{r}) = \sum_{n'}^N b_{n'} u_{n'\mathbf{k}_0}(\mathbf{r}) \quad (2)$$

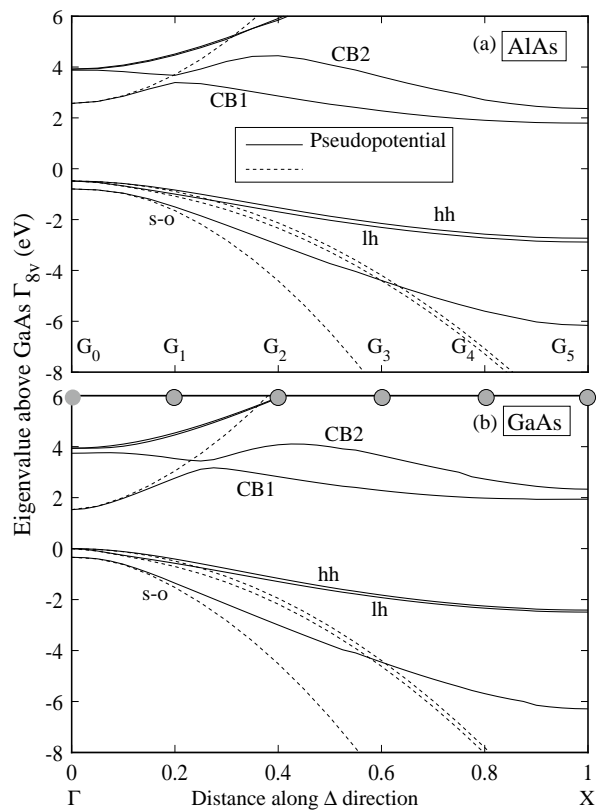
Choosing  $\mathbf{k}_0 = j$ , the  $u_{n\mathbf{k}}(\mathbf{r})$  obey [8]

$$\sum_{n'}^N \left\{ \left[ \epsilon_{n'}(j) - \epsilon_{n'}(\mathbf{k}) + \frac{\hbar^2 k^2}{2m} \right]^{-1} \mathbf{p}_{n',n'} \cdot \mathbf{k} \right\} b_{n'} = 0; \quad (3)$$

the effects of the microscopic crystal potential are now encoded in the  $\mathbf{p}_{n',n'} = \int \mathbf{p} u_{n'} \nabla u_{n'}^* d\mathbf{r}$ . Diagonalized with large enough  $N$ , eq. (3) would predict *full* (non-parabolic) bands throughout the zone, equivalent to direct solution of the Schrödinger equation for Bloch electrons [9]. The standard model [8], instead uses: i) *Degenerate perturbation theory*: For *bulk* semiconductors, the three valence states degenerate at  $j$  are usually augmented by the first conduction state. Including spin-orbit defines the 8-band  $k\phi$  model used below; ii) *Fitting*: The small  $N$  values ( $\lesssim 20$ ) in eq. (3) used in most  $k\phi$  calculations poorly describe band dispersion away from  $j$  if the  $\mathbf{p}_{n',n'}$  are actually computed from exact Bloch states  $u_{n'}(\mathbf{r})$ . The SM uses instead 'effective' matrix elements found [10] from measured gaps and band effective masses at  $j$ , mitigating the errors of i); iii) *Envelope functions*: To treat A/B *heterostructures*, the standard model generally uses the Luttinger-Kohn formalism [7] for response of a homogeneous crystal to a weak, *slowly-varying* external perturbation. The wave function in, *e.g.*, material A, takes the form

$$\psi(\mathbf{r}) = \sum_{n=1}^N F_n^A(\mathbf{r}) u_{n_j}^A(\mathbf{r}); \quad (4)$$

where the  $F_n^A(\mathbf{r})$  are 'envelope functions'. The  $u_{n_j}$  formally differ in A and B but virtually



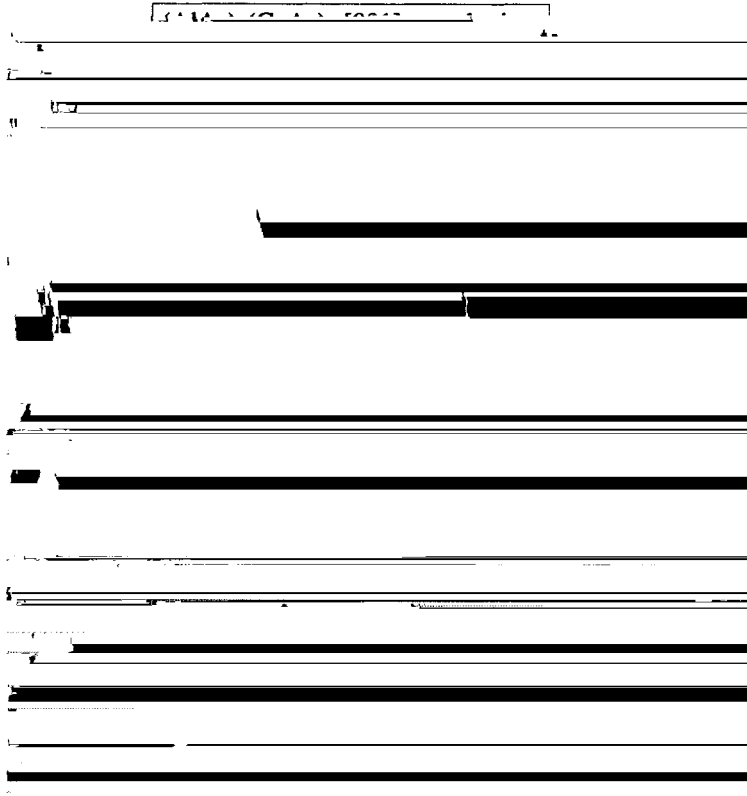


Fig. 2. { Band energies for [001] (AlAs)<sub>n</sub>(GaAs)<sub>n</sub> superlattices; *n<sub>c</sub>* indicates point of transition from indirect to direct gap system. Overbars indicate SL states which derive mainly from the ZB state in parentheses. Bulk ABP AlAs and GaAs band energies are given at right; the energy zero for *a*) and *b*) are bulk GaAs *j<sub>6c</sub>* and *j<sub>8v</sub>* states, respectively. Dashed lines show band connectivity near crossings, since *j* -*X* mixing is practically omitted.

*j* -like [14]. While the SM *X<sub>7v</sub>* GaAs valence state is almost 10 eV too low with respect to the pseudopotential value, the resulting error for heterostructure states is small because the pseudopotential *X<sub>7v</sub>* *j<sub>8v</sub>* valence band splitting is large (2.4 eV), so that interaction between heterostructure *j* - and *X*-derived valence states which fold to the heterostructure zone center is relatively weak.

Figure 2 compares zone-center ABP and SM band energies for [001] (AlAs)<sub>n</sub>(GaAs)<sub>n</sub> superlattices (SL) as a function of *n*. We label SL states via an overbar, with the ZB Brillouin zone point from which they derive in parentheses.  $\bar{j}(j)$  states derive principally from ZB *j* states, while  $\bar{j}(X_z)$  states derive mostly from folded-in zinc-blende *X<sub>z</sub>* states. Only the lowest  $\bar{j}(j)$  and  $\bar{j}(X_z)$  conduction and near-edge valence bands are shown. The extremely high energy of the SM bulk GaAs *X<sub>6c</sub>*

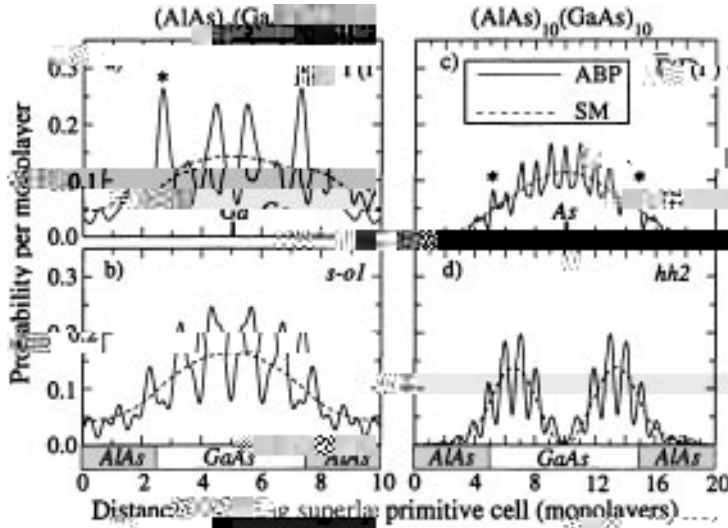


Fig. 3. { Square moduli of planar-averaged ABP Bloch states and SM envelope functions for  $\bar{j} (j)$  electron state and third hole state at  $\bar{j}$  for  $n = 5$  and  $n = 10$  SL. Odd (even)  $n$  superlattices have inversion symmetry about planes containing Ga (As) atoms. Note peaks on GaAs side of interfaces for electron states (asterisks).

ABP trends but place them *too deep* in energy; iii) for systems lacking inversion symmetry, lifting of the spin degeneracy away from the zone center is permitted in some directions. This spin splitting | absent in the SM | is significant ( $\gtrsim 30$  meV for the first heavy-hole state for  $\frac{q_{\perp} a}{2\pi} > 0.1$ ) for ‘in-plane’ dispersion in ABP calculations. SM band dispersion (not shown) agrees with ABP results only relatively near the SL zone center [13]. For  $n = 5$ , ABP values of  $m_k = m_{\gamma}$  at  $\bar{j}$  are, e.g.,  $\sim 3.4$  for the hh1 state and  $\sim 0.95$  for the  $\bar{j} (j_{6c})$  electron state, while SM values are 4.4 and 1.3, respectively; the anisotropy of effective masses is thus exaggerated within the SM. (GaAs) $_n$ /AlAs (1  $\cdot$   $n$   $\cdot$  10) quantum wells show [13]  $n_c \sim 9$  (cf. fig. 2), differences in valence band dispersion, and  $1 = n^2 \bar{j} (j)$  conduction band behavior to smaller  $n$  than for superlattices (fig. 2).

Figure 3 contrasts square moduli of ABP wave functions (full lines) averaged over transverse dimensions of the primitive cell to facilitate comparisons with SM envelope functions (dashed lines), for the  $\bar{j} (j)$  electron state and the third hole state at  $\bar{j}$ . Envelope functions for states whose energy (fig. 2) is well described by the SM closely average inner and outer envelopes of Bloch states. The  $n = 5 \bar{j} (j)$  ABP electron wave function shows interfacial peaks absent in the SM.

Projections of SL states onto zinc-blende states provide insight into why and where the SM fails. [001] (AlAs) $_n$ (GaAs) $_n$  superlattice states at  $\bar{j}$  derive from ZB states at the SL reciprocal lattice vectors  $G_j = \frac{2\pi j}{na}$  for  $j = 0; 1; 2; \dots; n$  along the [001]  $j$ -X ( $\Phi$ ) line. We may thus expand a  $\bar{j}$  SL state in a complete set of ZB Bloch states at these  $G_j$ :

$$j \hat{i}^{\text{SL}} = \sum_s \sum_{G_j=j}^{\times} f_{s;G_j} j \hat{i}^{\text{ZB}}_{s;G_j} \tag{5}$$

the  $G_{j \neq 0}$  (gray circles for (AlAs) $_5$ (GaAs) $_5$  in fig. 1) fold to  $\bar{j}$  in the SL geometry. The projection of a specified SL state onto zinc-blende band  $s$  at  $G_j$  is thus  $P_{s;G_j} \cdot j \hat{i}^{\text{SL}} \cdot j \hat{i}^{\text{ZB}}_{s;G_j} =$

Table I. { Projections  $P_{sG_j}$  of ABP near-edge  $(\text{GaAs})_5(\text{AlAs})_5$  states at  $\bar{j}$  ('State') onto GaAs band  $s$  labeled 'On' at the  $G_j = \frac{2\pi j}{5a}$ , and net projection  $P_s$  on band  $s$ .  $G_0$  and  $G_5$  correspond to ZB  $j$  and  $X$  points, respectively.

State	On	$G_0$	$G_1$	$G_2$	$G_3$	$G_4$	$G_5$	$P_s$
$\bar{j}(j)$	CB1	0.80	0.08	0	0.05	0.02	0	0.94
$\bar{j}(X_z)$	CB1	0	0	0.00	0.00	0.03	0.95	0.99
'hh1'	hh	0.84	0.15	0.00	0.00	0	0	1.00
'lh1'	lh	0.93	0.06	0	0	0	0	0.98
's-o1'	s-o	0.80	0.01	0	0	0	0	0.81
'hh2-a'	hh	0	0.89	0.04	0	0	0	0.93
'hh2-b'	hh	0.14	0.81	0.02	0.00	0	0	0.97
'lh2-a'	lh	0	0.93	0.02	0	0	0	0.95
'lh2-b'	lh	0.04	0.78	0.01	0	0	0	0.83

$= \sum_{s,G_j} P_{sG_j}$ . The net contribution  $P_s \cdot \sum_{j=0}^n P_{sG_j}$  measures how completely the SL state derives from ZB band  $s$ . Similarly, the quantity  $P \cdot \sum_{s=1}^{N_b} P_s$  measures how nearly the finite set of  $N_b$  zinc-blende bands used is 'complete' ( $P \cdot 1$ ), *i.e.* adequately describes the specified SL state.

For near-edge ABP  $(\text{AlAs})_5(\text{GaAs})_5$  superlattice states table I shows the projections  $P_{sG_j}$  onto the (spin-split) first conduction band CB1 and hh, lh, and s-o valence bands (1) | the same set used by the 8 £

high in energy: fig. 1) are important (table I) and SM predictions *must* be too high (fig. 2) until the shortest  $G_j$  move into the CB1 quadratic region. As the period  $n$  increases, points along the zinc-blende  $\phi$  direction which fold to  $\bar{j}$  move into the region where  $k\phi$  adequately represents the bulk zinc-blende band structures and all near-edge superlattice states will be well described by the 'standard model'.

We have thus traced errors in the  $k\phi$ +EFA approach to poor  $k\phi$  description of dispersion of *bulk* bands which are mixed in heterostructure states. The 8-band  $k\phi$  approach correctly focuses on four spin-split *bands*, but fails to keep enough ( $N$  in eq. (3)) zone-center *states* to adequately describe their dispersion for thin heterostructures. For  $\text{Ga}_x\text{In}_{1-x}\text{P}$  ordered alloys [16] zinc-blende states along the [111]  $j$ - $L$  direction fold and couple, so the SMs inadequate description of the bulk  $L$  point will cause errors similar to those for [001] superlattices. The central issue is not the heterostructure thickness *per se*, but whether off- $j$  bulk states poorly described by the 'standard model' are significantly mixed (as determined by the proximity in energy of bulk zinc-blende  $L$ ,  $j$ , and  $X$  states) in heterostructure bands.

\*\*\*

We thank K. Mäder and R. Maurer for useful discussions and suggestions, A. Franceschetti and L.-W. Wang, and S. Froyen for suggestions about heterostructure state projections and the conjugate gradient program. This work was supported by the Office of Energy Research, Materials Science Division, US DOE grant DE-AC36-83CH10093, and the Israel Science Foundation, administered by the Israel Academy of Sciences and Humanities.

#### REFERENCES

- [1] Wang L.-W. and Zunger A., *J. Phys. Chem.*, **98** (1994) 2158; *Phys. Rev. Lett.*, **73** (1994) 1039; *J. Chem. Phys.*, **100** (1994) 2394; Mäder K. M., Wang L.-W. and Zunger A., *Phys. Rev. Lett.*, **74** (1995) 2555.
- [2] Fasol G., Fasolino A. and Lugli P. (Editors), *Spectroscopy of Semiconductor Microstructures*, NATO ASI Ser. B., Vol. **206** (Plenum Press, New York, N.Y.) 1989.
- [3] See, e.g., Bastard G., Brum J. A. and Ferreira R., in *Solid State Physics*, edited by D. Turnbull and H. Ehrenreich, Vol. **44** (Academic, New York, N.Y.) 1991, p. 229.
- [4] See, e.g., Alonso M.-I., Ilg M. and Ploog K. H., *Phys. Rev. B*, **50** (1994) 1628.
- [5] Burt M. G., *J. Phys. Condens. Matter*, **4** (1992) 6651.
- [6] Smith D. L. and Mailhot C., *Rev. Mod. Phys.*, **62** (1990) 173.
- [7] Luttinger J. M. and Kohn W., *Phys. Rev.*, **97** (1955) 869.
- [8] Kane E. O., in *Handbook on Semiconductors*, edited by T. S. Moss, vol. 1 (North Holland, Amsterdam) 1982 Chapt. 4A, pp. 193-217.
- [9] Cardona M. and Pollak F. H., *Phys. Rev.*, **142** (1966) 530; Cardona M., Christensen N. E. and Fasol G., *Phys. Rev. B*, **38** (1988) 1806.
- [10] Baraff G. A. and Gershoni D., *Phys. Rev. B*, **43** (1991) 4011. See also Gershoni D., Henry C. H. and Baraff G. A., *IEEE J. Quantum Electron.*, **29** (1993) 2433.
- [11] Winkler R. W. and Rössler U., *Phys. Rev. B*, **48** (1993) 8918.
- [12] Mäder K. A. and Zunger A., *Phys. Rev. B*, **50** (1995) 17393.
- [13] Wood D. M. and Zunger A., *Phys. Rev. B*, **53**, 15 March 1996.
- [14] Edwards G. and Inkson J. C., *Solid State Commun.*, **89** (1994) 595 review  $j$ - $X$  mixing in heterostructures and other deficiencies of the EFA.
- [15] Wei S.-H. and Zunger A., *J. Appl. Phys.*, **63** (1988) 5794.
- [16] Franceschetti A., Wei S.-H. and Zunger A., *Phys. Rev. B*, **52** (1995) 13992.